AD-A162 335 THE TURBULENT GRAVITY WAVE-CRITICAL LEVEL ENCOUNTER IN THE EVOLUTION OF A (U) GOULD DEFENSE SYSTEMS INC MIDDLETOWN RI OCEAN DEFENSE DIV J R GRANT JUN 85 1/1

UNCLASSIFIED OSD-771-HYDRO-CR-85-03 AFOSR-TR-85-1006 F/G 4/1 ML

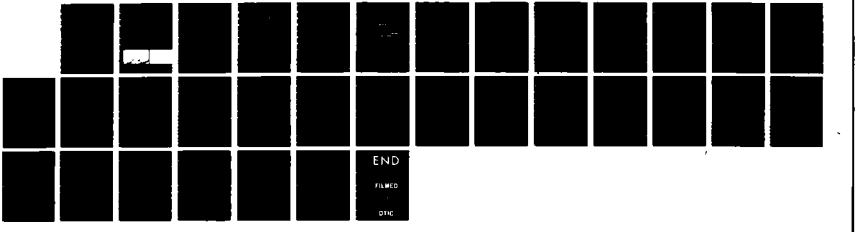

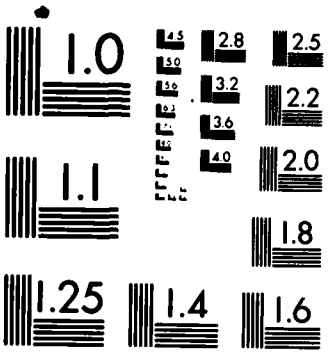

THE TURBULENT GRAVITY WAVE-CRITICAL LEVEL ENCOUNTER IN THE EVOLUTION OF ATMOSPHERIC FLOW

REPORT FOR 1984-85

~~AFOSR CONTRACT NUMBER~~

~~N00014-84-C-0046~~

GOULD

HYDRODYNAMICS RESEARCH

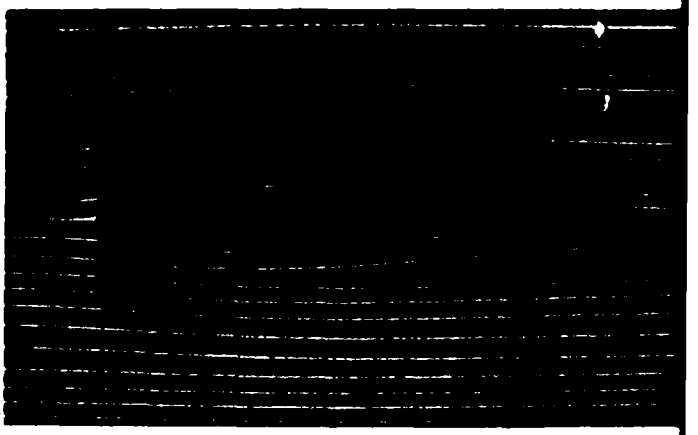

ASW SYSTEMS ENGINEERING FACILITY • NEWPORT, RHODE ISLAN

OSD-771-HYDRO-CR-85-03

THE TURBULENT GRAVITY WAVE-CRITICAL LEVEL ENCOUNTER IN THE EVOLUTION OF ATMOSPHERIC FLOW

REPORT FOR 1984-85

JOHN R. GRANT

GOULD DEFENSE SYSTEMS, INC.
Ocean Systems Division
One Corporate Place
Newport Corporate Park
Middletown, RI 02840

JUNE 1985

submitted to

Lt. Col. Gerald J. Dittberner
Program Manager
Directorate of Chemical and Atmospheric Sciences
Air Force Office of Scientific Research
Bolling Air Force Base, DC 20332

AFOSR CONTRACT No. 49620-84-C-0048

UNCLASSIFIED

SECURITY CLASSIFICATION OF THIS PAGE

AD-A162 335

REPORT DOCUMENTATION PAGE

1a. REPORT SECURITY CLASSIFICATION: Unclassified	1b. RESTRICTIVE MARKINGS
2a. SECURITY CLASSIFICATION AUTHORITY	3. DISTRIBUTION/AVAILABILITY OF REPORT: Approved for public release Distribution unlimited
2b. DECLASSIFICATION/DOWNGRADING SCHEDULE	
4. PERFORMING ORGANIZATION REPORT NUMBER(S)	5. MONITORING ORGANIZATION REPORT NUMBER(S): AFOSR-TR- 85-1006
6a. NAME OF PERFORMING ORGANIZATION: Gould Defense Systems, Inc. / 6b. OFFICE SYMBOL (If applicable)	7a. NAME OF MONITORING ORGANIZATION: AFOSR/NC
6c. ADDRESS (City, State and ZIP Code): Ocean Systems Division, One Corporate Place, Newport Corporate Park, Middletown, RI 02840	7b. ADDRESS (City, State and ZIP Code): Bldg 410, Bolling AFB, DC 20332-6448
8a. NAME OF FUNDING/SPONSORING ORGANIZATION: AFOSR / 8b. OFFICE SYMBOL (If applicable): NC	9. PROCUREMENT INSTRUMENT IDENTIFICATION NUMBER: F49620-84-C-0048
8c. ADDRESS (City, State and ZIP Code): Bldg 410, Bolling AFB, DC 20332-6448	10. SOURCE OF FUNDING NOS.

PROGRAM ELEMENT NO.	PROJECT NO.	TASK NO.	WORK UNIT NO.
61102F	2310	A1	

11. TITLE (Include Security Classification): The Turbulent Gravity Wave-Critical Level Encounter in the Evolution of Atmospheric Flows

12. PERSONAL AUTHOR(S): John R. Grant

13a. TYPE OF REPORT	13b. TIME COVERED	14. DATE OF REPORT (Yr., Mo., Day)	15. PAGE COUNT
Final	FROM _____ TO _____	June 1985	29

16. SUPPLEMENTARY NOTATION

17. COSATI CODES			18. SUBJECT TERMS (Continue on reverse if necessary and identify by block number)
FIELD	GROUP	SUB. GR.	turbulent gravity, doppler radars, atmosphere

19. ABSTRACT (Continue on reverse if necessary and identify by block number)

See other side----

20. DISTRIBUTION/AVAILABILITY OF ABSTRACT	21. ABSTRACT SECURITY CLASSIFICATION
UNCLASSIFIED/UNLIMITED ☐ SAME AS RPT. ☐ DTIC USERS ☐	UNCLASSIFIED

22a. NAME OF RESPONSIBLE INDIVIDUAL	22b. TELEPHONE NUMBER (Include Area Code)	22c. OFFICE SYMBOL
Francis J. Wodarczyk	767-4963	NC

DD FORM 1473, 83 APR EDITION OF 1 JAN 73 IS OBSOLETE.

Unclassified

SECURITY CLASSIFICATION OF THIS PAGE

ABSTRACT

The extended objective of this work is to contribute to the understanding of the short term response of the atmosphere to forcing by turbulent gravity wave-critical level encounters. A combination of numerical and observational approaches is used.

Several nonturbulent and turbulent calculations of a gravity wave-critical level encounter have been performed. Examples are discussed. Those calculations including turbulence are noteworthy in that they are the first known. However, numerical difficulties associated with the level 2 turbulence model of the code have prevented the computation of the encounter to sufficiently late times. A new code, employing a level 4 model, is now being developed through support from the National Science Foundation. Early efforts in the upcoming year will include completion of the numerical calculations using the new code.

The simulated signatures will aid in the examination of interpretation of the records of the Poker Flats and Sunset doppler radars. Of those events which can be identified as critical level encounters, one or two will be selected for numerical simulation, for which key parameters are matched to those extracted from the observations. Even order-of-magnitude agreement between observed and calculated C_n^2 time series would lend quantitative significance to this work, which would extend to the calculated modifications of the mean flow.

A second point of interaction with observations is the internal wave experiments proposed to be performed at the annular tank facility at Physical Dynamics, Inc. Numerical simulation of one of these experiments will provide an opportunity to evaluate the turbulence model as well as the overall calculational procedure. As with the interaction with the Doppler radar data, this collaboration will allow both a test of the numerics and an enhancement of the data interpretation.

DISCLAIMER NOTICE

THIS DOCUMENT IS BEST QUALITY PRACTICABLE. THE COPY FURNISHED TO DTIC CONTAINED A SIGNIFICANT NUMBER OF PAGES WHICH DO NOT REPRODUCE LEGIBLY.

TABLE OF CONTENTS

ABSTRACT

The extended objective of this work is to contribute to the understanding of the short term response of the atmosphere to forcing by turbulent gravity wave-critical level encounters. A combination of numerical and observational approaches is used.

Several nonturbulent and turbulent calculations of a gravity wave-critical level encounter have been performed. Examples are discussed. Those calculations including turbulence are noteworthy in that they are the first known. However, numerical difficulties associated with the level 2 turbulence model of the code have prevented the computation of the encounter to sufficiently late times. A new code, employing a level 4 model, is now being developed through support from the National Science Foundation. Early efforts in the upcoming year will include completion of the numerical calculations using the new code.

The simulated signatures will aid in the examination of interpretation of the records of the Poker Flats and Sunset doppler radars. Of those events which can be identified as critical level encounters, one or two will be selected for numerical simulation, for which key parameters are matched to those extracted from the observations. Even order-of-magnitude agreement between observed and calculated C_n^2 time series would lend quantitative significance to this work, which would extend to the calculated modifications of the mean flow.

A second point of interaction with observations is the internal wave experiments proposed to be performed at the annular tank facility at Physical Dynamics, Inc. Numerical simulation of one of these experiments will provide an opportunity to evaluate the turbulence model as well as the overall calculational procedure. As with the interaction with the Doppler radar data, this collaboration will allow both a test of the numerics and an enhancement of the data interpretation.

1. INTRODUCTION

The extended objective of this work is to contribute to the understanding of the short term response of the atmosphere to short term influences. The particular influence studied is internal gravity wave motion, specifically the encounter of a gravity wave with a critical level, a height where the component of the wind speed in the direction of horizontal phase propagation matches the horizontal component of wave phase speed. Two major effects of such encounters are the deposition in the wind of momentum transported by the wave motion and the generation of turbulence by the wave motion. Both phenomena modify the wind in the vicinity of the critical level.

As discussed in the original proposal, the former effect has been studied by a number of investigators, and the present work builds on their results. The explicit inclusion of turbulence generated by the wave motion is a new feature.

The approach of this study is to combine the results of numerical simulations with observations produced by Doppler radar to understand the form of the atmospheric response to these effects, the details of the physics of the various processes involved, and the magnitude of the response under various typical conditions. This combination can be productive since the radar records may display wave motion and indications of strength of turbulence activity, which are the features of the numerical simulations.

The first year's work has concentrated on performing several numerical simulations of the turbulent gravity wave-critical level encounter. Results are presented in the following sections. In the second year I plan to

examine radar records from the Poker Flats and Sunset radars in view of the first year's calculations. I also would collaborate on wave-critical level tank experiments proposed to be performed at Physical Dynamics, Inc. These plans are discussed more fully in the fourth section.

2. GENERAL DISCUSSION OF THE PROGRESS

The milestones achieved this year are:

1. The Fortran code was re-assembled to run on the AFWL Cray-1 and carefully validated against previous output. [This step was necessary because the only version available to me was one running on a VAX 11/780 (host)-FPS 164 (array processor) combination, which requires a specialized, machine-dependent form.]
2. The existing "level 2" turbulence model for the Reynolds stresses was replaced by the more widely used (and hence accepted) "level 2" model of Gibson and Launder (1976).
3. The existing rigid wall boundary conditions on the left and right edges of the computational domain of the code were replaced by periodic boundary conditions. [Numerical difficulties led to the discovery that this step also requires a second level of iteration on the successive over-relaxation (SOR) pressure solver.]
4. The existing rigid wall boundary conditions at the lower edge of the computational domain were replaced by a wave-forcing boundary condition. [Numerical instabilities resulted from this step. The cure was achieved by specifying a background wind which was zero at this boundary.]
5. A variety of runs were made simulating a gravity wave-critical level encounter.

The particulars of some of these runs are presented in the next section. Those including turbulence calculations are noteworthy because they are the only ones to date to do so. However, they extend to only a half-period or so beyond the point of wavebreaking. A stong numerical

instability associated with the turbulent vertical mass flux has prevented lengthier calculations. Such behavior is not uncommon with level 2 turbulence models, and could be remedied with one or two months intensive effort (perhaps using techniques employed for a somewhat similar situation by B. Launder, private communication). [In a level 2 model, the assumption of relatively small anisotropy is made, which allows the dropping of the temporal and spatial derivatives in the original equations. The differential equations thus are reduced to algebraic equations.]

However, I have decided on another course to produce the desired numerical calculations, because of a recent development. In conjunction with Dr. John T. Merrill at the University of Rhode Island, I have been awarded a grant by NSF (Meteorology) to develop and use a code designed specifically for studying wave-turbulence interactions, of which gravity wave-critical level encounters are one example. Briefly, the wind and wave portions of the flow are spectrally decomposed in the horizontal, finite-differenced in the vertical, and the turbulence correlations are computed by a level 4 model. [In the level 4 model, the only approximations made to the exact equations are the expressions or "closures" used for the unknown correlations - all time and space derivations are kept.] Hence the turbulence can be much more responsive to the evolving wave motion, and calculated under far less drastic assumptions. This code is now being developed. Accordingly, instead of spending more time on the existing code, I have decided that, for this work, it will be more profitable to use that time on the new code. After its validation, I will immediately use it to complete this phase of the turbulent gravity wave-critical level interaction. I anticipate completion by the beginning of FY86.

The existing code has been exhaustively validated, so its computational results will be a valuable aid in validating the new code. In addition, the experience gained performing the calculations described next already has been quite useful in developing the new code.

3. SPECIFIC CALCULATIONAL RESULTS

3.1 NONTURBULENT CALCULATIONS

Results of a nonturbulent (i.e., turbulence model turned off) calculation are shown in Figures 1 and 2. The wind is described by

$$\bar{u}(z) = \tanh(z) - \tanh(z_b).$$

so that distance is scaled on shear layer half-thickness and velocity is scaled on half the velocity change across the shear layer. The height z_b is the (scaled) height of the bottom of the computational domain. The top is at $z = z_t$ and for this calculation I use

$$z_b = -1.5$$
$$z_t = 1.2$$

The background stratification is uniform:

$$\bar{\rho}(z)/\rho_o = 1.0 + Ri_m \, z/g_*$$

where ρ_o is the density at the critical level and g_* is the nondimensional acceleration due to gravity. The minimum Richardson number is $Ri_m = 2.0$. With Ri_m specified, setting the value of g_* requires specification of two of the three quantities: height scale, velocity scale, or Brunt-Vaisala frequency. I have chosen $N = 0.01$ sec^{-1} and the velocity scale to be 5 m/sec, so that the height scale is 707 meters and $g_* = 277$.

The wave is forced at the bottom of the computational domain by requiring

$$w(x, z_b, t) = A(t) \sin (kx + mz_b - \omega t)$$

where

$$A(t) = \begin{cases} A_o t/T & , t \leq T \\ A_o & , t > T \end{cases}$$

with the other computational variables given by the usual polarization relations. Here $A_o = 0.1$ is taken, and $T = 6\pi/\omega$. The wave frequency is set by

$$\omega = \{Ri_m/[1 + (m/k)^2]\}^{1/2}$$

and for this run the local vertical wavenumber m at $z = z_b$ is chosen to be related to the horizontal wavenumber k by

$$m/k = -1$$

so that $\omega = 0.5$.

The horizontal wavenumber is specified by

$$k = \omega/\bar{u}(z = 0)$$

$$= \omega/\tanh(|z_b|)$$

so that the critical level (except for the startup transients) lies at $z = 0$. The horizontal domain extends from

$$x_{min} = -\pi/k$$

$$x_{max} = \pi/k + \Delta x$$

where Δx is the horizontal distance between neighboring computational points (the extra cell is added to allow the proper enforcement of the periodic boundary conditions).

The boundary condition at the top of the domain is the free-slip condition at a rigid wall. The number of computational points in the horizontal is 42, and the number in the vertical is 41, for a total of 1722.

The critical level is at z=0, which in Figures 1 and 2 is row 25 of the matrix. The flow is entirely horizontal at t=0, when the wave is begun to be forced at the lower boundary (row 1 of the matrix). In order to maintain a reasonably-sized number of computational points yet resolve the gradients in the vicinity of the critical level, the mesh is stretched. The physical spacing between points in the vertical as the critical level is only 1/3 the vertical spacing at the lower boundary.

To produce these figures, the calculational arrays themselves have been printed out after being normalized by their maximum values. Hence a "53" means 53% of the maximum found on the array at this time step. Since the print-out on the page is uniform in the vertical, the mesh stretching is not accounted for. Hence the displayed fields are distortions of the physical fields. To see the effect of this distortion, Figure 1(a) should be compared with Figure 3(a), which was computed using a uniform computational

mesh, and thus has no distortion. Even with this distortion in Figure 1 and 2, however, the main results are clearly evident, and they do have the benefit of displaying the details near the critical level.

Figure 1 displays the component of wave-associated velocity along the direction of the wind at the times of 3.5, 4.0, 4.5, and 5.0 wave periods after the start of the calculation. (Note the propagation of the wave phase about 1/2 wavelength--or half the horizontal distance shown on the plot--from one plot to the next). The major features visible are:

1. The wave is not penetrating the critical level.
2. The wave motion in the direction of the wind is increasing, and the motion against the wind is decreasing (note the near absence of negative values in Figure 1(d)).
3. Since heavier air thus is being carried over lighter, the wave breaks. [This breaking has just begun in 1(a). Notice the downward trend in the peak velocity, indicated by ***, from one plot to the next, and the build up of the strong gradient below the peak as the air falls].
4. By 5 wave periods (Figure 1(d)), the original well-ordered, nearly linear wave has taken on a complex, highly nonlinear form.

Figure 2 shows the effect of this motion on the density (or temperature) field. Here the total density ρ is plotted in the form ρ/ρ_0-1. At the initial time (t=0), these density contours were horizontal. At this time (5 wave periods into the simulation), there are several large regions where heavier air overlays lighter.

Certainly when such an encounter occurs in nature, a substantial amount of turbulence will be generated. This turbulence will help absorb the wave

into the flow. Noticing from, say, Figure 1(d), that the wave has a large mean velocity component in the direction of the flow, we conclude that such an event will significantly alter the wind field in the height vicinity of the critical level.

3.2 TURBULENT CALCULATIONS

The preceding results indicate the value (perhaps necessity) of performing studies of critical level encounters which include turbulence in the study, if realistic assessments of such encounters are to be made. Figure 3 displays the results of one such calculation. All of the parameters (background, mesh size, etc.) are the same, except the mesh is not stretched, so that is no distortion of the wave fields in these plats.

The intent in choosing initial conditions for the turbulence variables is simply to pick values which are small enough not to affect the initial evolution of the flow, but not so small that growth to reasonable values could be delayed. I have used for this run

$$q = 10^{-4}.$$

As a guide in setting a reasonable corresponding dissipation rate, I have used the observation that in equilibrium shear layer turbulence the time scale is about three times the inverse of the maximum shear, setting

$$e = 0.3\ q\ \frac{d\bar{u}}{dz}\Big|_o = 0.3\ q\ .$$

In Figure 3(a) is shown the wave-associated velocity component in the direction of the wind (as in Figure 1) at 3 wave periods after initialization. The turbulence intensity is shown in Figure 3(b). The wave has not

yet started breaking, and this turbulence is due to the strong shear developing between wave phases as the critical level is approached. The result is a very thin layer just below the critical level, strongly dependent on wave phase. From the nonturbulent results in Figures 1 and 2, the wave will soon break. This should result in the rapid appearance of turbulence distributed, according to Figure 2, over a much thicker region.

An effect of stratification can be seen by comparing Figure 3 and 4. In this latter figure, the Brunt-Vaisala frequency has been halved, so the Richardson number is reduced from 2.0 to 0.5. The time of Figure 4 is 2.2 wave periods, slightly earlier than that of Figure 3 (which is 3 periods). Also, the mesh is much finer. The number of computational points in the horizontal is 82, and the number in the vertical is 91, for a total of 7462.

Notice the broader appearance of the wave as the critical level is approached. Also, the turbulence intensity is spread over a thicker layer. As with Figure 3, this turbulence is due to shear production; the wave has just approached the point of breaking and rapidly generating an active turbulence region.

In both of these cases, the level 2 turbulence model has not been able to follow this generation. Hence, as discussed, I am going to a level 4 code. The new code should provide a reliable and unique tool for examining this way of modifying the atmospheric flow.

4. PLANS FOR THE NEXT YEAR

The research effort in the upcoming year will be two-fold in approach, employing both numerical and observational techniques. The new code will be used to perform at least two simulations similar to those depicted in the figures, but well into the mature, breaking stage of the encounter. Analysis of these runs will include (the notation is that of the original proposal)

1. Comparison of the shape and magnitude of the height profile of the momentum fluxes $\overline{\tilde{u}\,\tilde{w}}$ and $\overline{u'w'}$ and density fluxes $\overline{\tilde{\rho}\,\tilde{w}}$ and $\overline{\rho'w'}$.
2. Comparison of the height profiles of the height derivatives of these quantities, which is what modifies the wind.
3. Investigation of the relation, particularly in phase, of the wave-induced turbulent momentum fluxes, $\tilde{r}_{ij}$ and the wave strain rates $\partial\tilde{u}_i/\partial x_j$, since these quantities determine the rate of exchange of energy between the wave and turbulent fields.
4. Study of the behavior and location of turbulence intensity and production versus that of the total (wind-plus-wave) Richardson number.
5. The effect of turbulence as revealed by contrasting these calculations with previous laminar calculations performed by others (ideally, this should be done by a comparison of laminar results produced by this code for otherwise identical runs, but limited resources may require focusing on the turbulent runs).
6. Inspection of the behavior of the turbulence diffusivity and Prandtl number.

For part of the observational work, these results will be used to characterize the signature such an encounter would produce in Doppler radar records. In considering a suitable parameter with which to characterize the signal, the refractivity structure constant C_n^2 is a first choice. This quantitiy can be computed from the turbulent volume reflectivity η_t by

$$C_n^2 = \eta t \, \lambda_r^{1/3} / 0.38,$$

where λ_r is the radar signal wavelength. For a given radar geometry and operating condition, the volume reflectivity may be computed from the relative echo strength using the radar equation.

Note that C_n^2 has the advantage, once computed from the data, of being independent of the attributes of any given radar. As such, this quantity is a useful point of confluence of the range-gated radar return signal strength records and the numerical calculations.

I derived in the second year proposal (February, 1985) a relation between C_n^2 and the turbulence dissipation rate ε:

$$C_n^2 \sim (\phi/q) \, \varepsilon^{2/3}$$

where q is the turbulence intensity and ϕ is the relative variance of mass density (this latter term will include variance in electron number

density at heights where free electrons contribute to the electromagnetic index of refraction). All of the quantities on the right in this expression, and thus C_n^2, will be routinely computed in the simulations.

Prominent features of the simulated signatures will include the magnitude and phase of wave-induced fluctuations in, C_n^2 relative to the magnitude and phase of the radial (along-the-beam) component of wave-associated velocity, and the geometrical form of the mean and wave-induced fluctuations of C_n^2, scaled by shear layer thickness. The signatures will be displayed for a sequence of times as the encounter evolves.

The first use of the simulated signatures will be as a pattern with which to examine and interpret the available radar records. From the set of critical level events identified in the data, one or two will be chosen for further calculational investigation. One or possibly several simulations will be performed in which are matched as many key parameters (e.g., wavelength-to-shear layer thickness, incoming wave amplitude-to-wind-speed difference across the shear layer, ambient turbulence levels, minimum Richardson number) as can be extracted from the data set. The degree of unambiguity in the radar record, and the amount and quality of supporting data (e.g., a recent nearby rawinsonde, clear observation of the wave motion by a neighboring microbarograph array) will be prime criteria in this choice of events. If this second tier of simulations can produce C_n^2 signatures which are similar in form and whose magnitude is within, say, an order of magnitude of the observation, then the step from idealized depiction toward

quantitative significance would at least have been begun. This step would extend to the computed modification of the wind by the wave and turbulence fields, a central point of investigation. Finally, if a particularly clear case (e.g., comparable to the third shear-generation event discussed by Grant, 1979) can be located, some inferences about the C_n^2 calculation, and indeed, the turbulence model itself, may be able to be drawn.

A six foot diameter annular tank is now being tested at Physical Dynamics, Inc. Bellevue, Washington. This facility will have unique capabilities for the observation of wave pheonomena on relatively long time scales. Part of its use to be proposed for the upcoming year is to study wave - critical level encounters, including breaking cases (Dr. D. Delisi, private communication). Such experiments will provide valuable points of comparison with numerical studies. Particularly noteworthy will be the opportunity to evaluate the computed turbulence field against controlled observations. Consequently, I will carefully simulate one of the wavebreaking, critical level encounters to be performed in this tank. As with the interaction with the Doppler radar measurements, such collaboration of results will allow both testing of the calculations and enchanced interpretation of the observations.

FIGURE CAPTIONS

FIGURE 1. Contours of the wave-associated velocity component along the wind, for a nonturbulent calculation. The horizontal distance (one wavelength) shown is 5.5 and the vertical distance is 2.7 (distances are normalized by the half-thickness of the shear layer). The critical level is indicated by an arrow. The mesh is stretched in the vertical, so the spacing between computational points at the critical level is 1/3 that as the lower boundary. The times shown are 3.5(a), 4.0(b), 4.5(c), and 5.0(d) wave periods after start-up. Contours are at $\pm$ 20, 40, 60, 80% of maximum.

FIGURE 2. Contours of the total (background plus wave) density ρ (displayed as ρ/ρ_0-1, were ρ_0 is the density at the critical level), from the calculation shown in Figure 1, at t=5.0 wave periods. Contours are at 10, 20, ..., 90% of maximum.

FIGURE 3. Contours of (a) the wave-associated velocity component along the wind and (b) the turbulence intensity (or kinetic energy per unit mass), as t=3.0 wave periods. As in Figures 1 and 2, the minimum background Richardson number is 2.0. The computational mesh is uniform. Contours are at $\pm$ 20, 40, 60, 80% of maximum.

FIGURE 4. Contours of (a) the wave-associated velocity component along the wind and (b) the turbulence intensity, as t=2.2 wave periods. The minimum background Richardson number is 0.5 (i.e., density stratification is half that of the previous figures). The nondimensional horizontal distance shown (one wavelength) is 12.05, and the vertical is 3.0. In (a), contours are at $\pm$ 20, 40, 60, 80% of maximum; in (b), contours are at 10, 30, 50, 70, 90% of maximum.

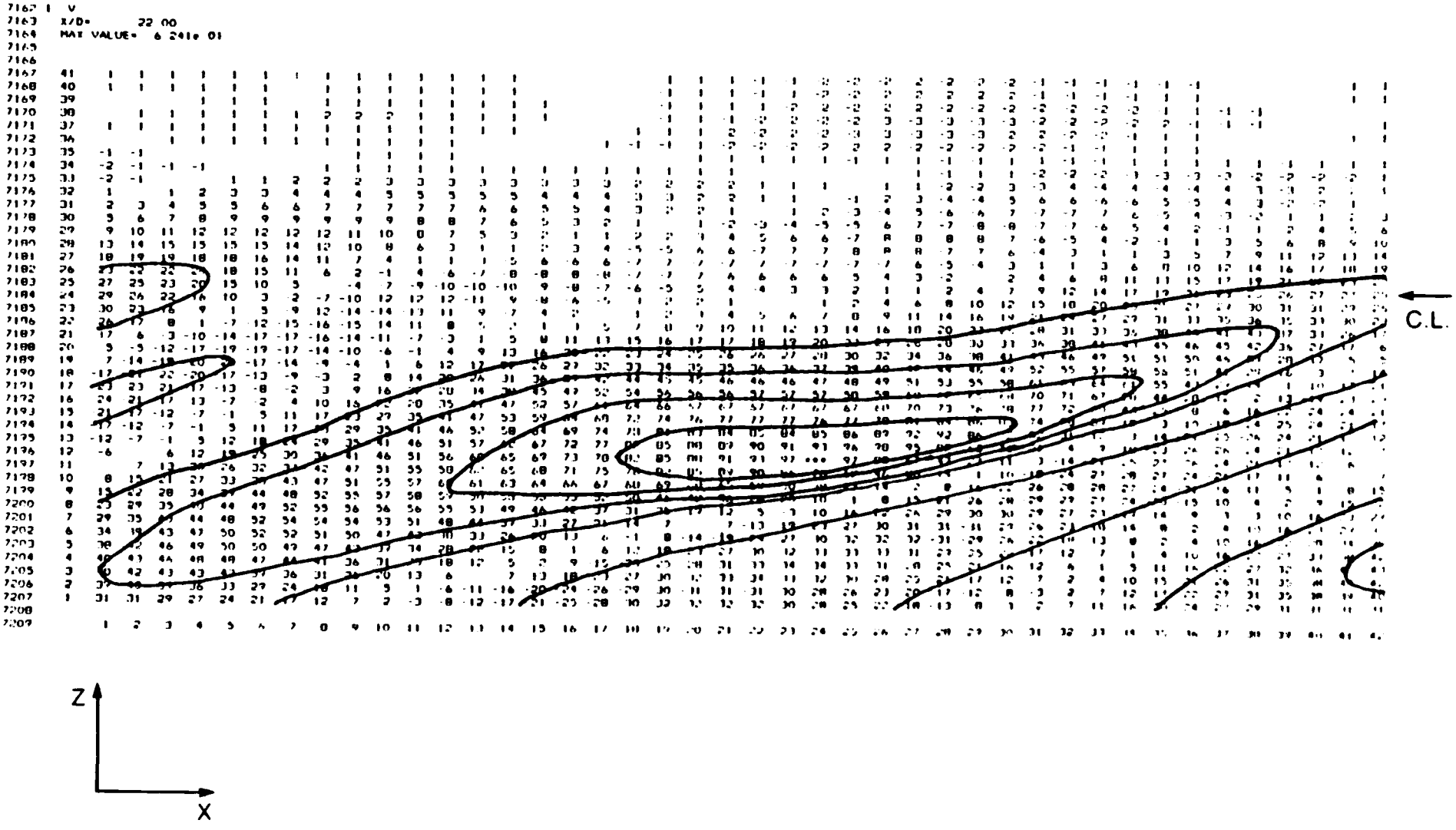

FIGURE 1(a)

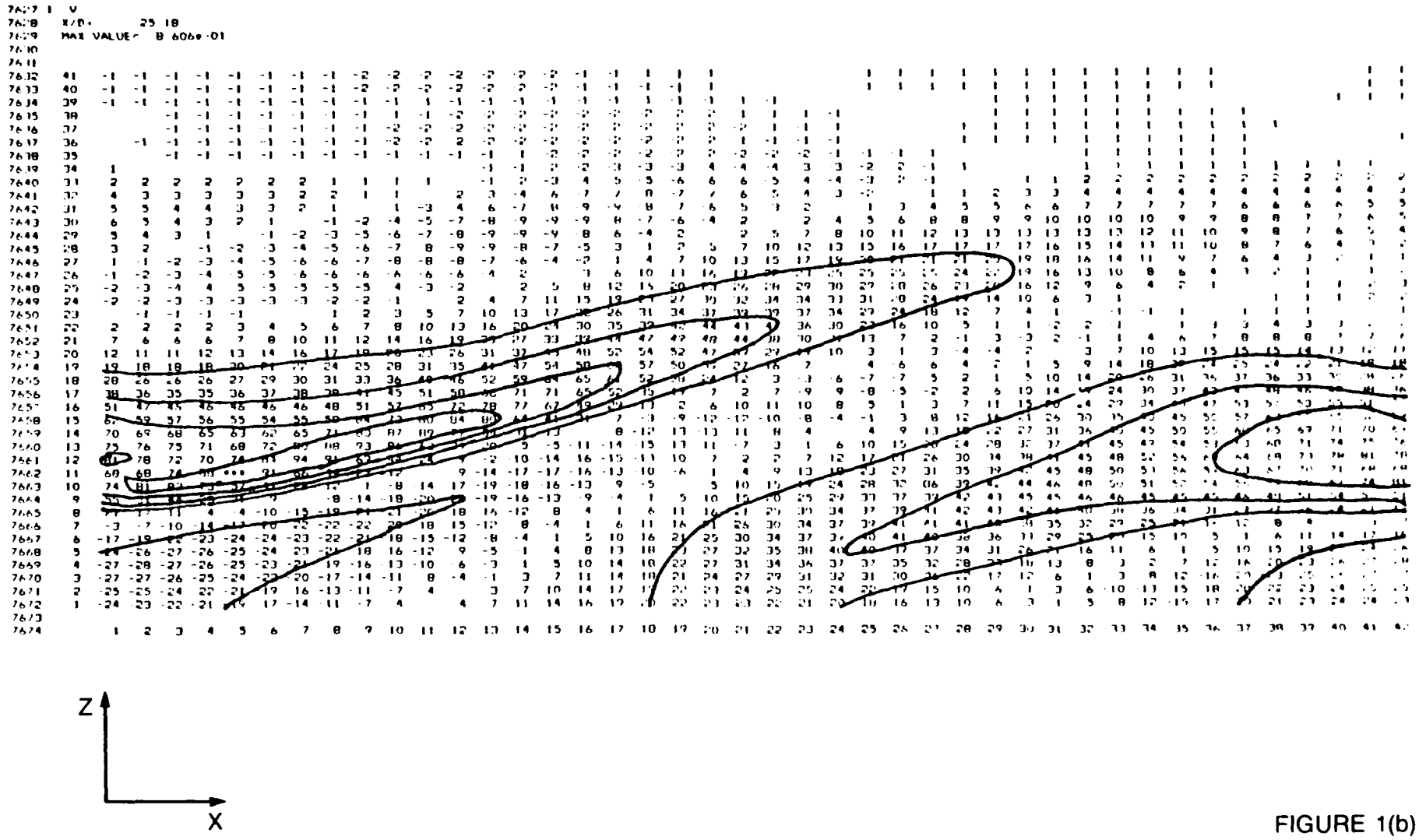

FIGURE 1(b)

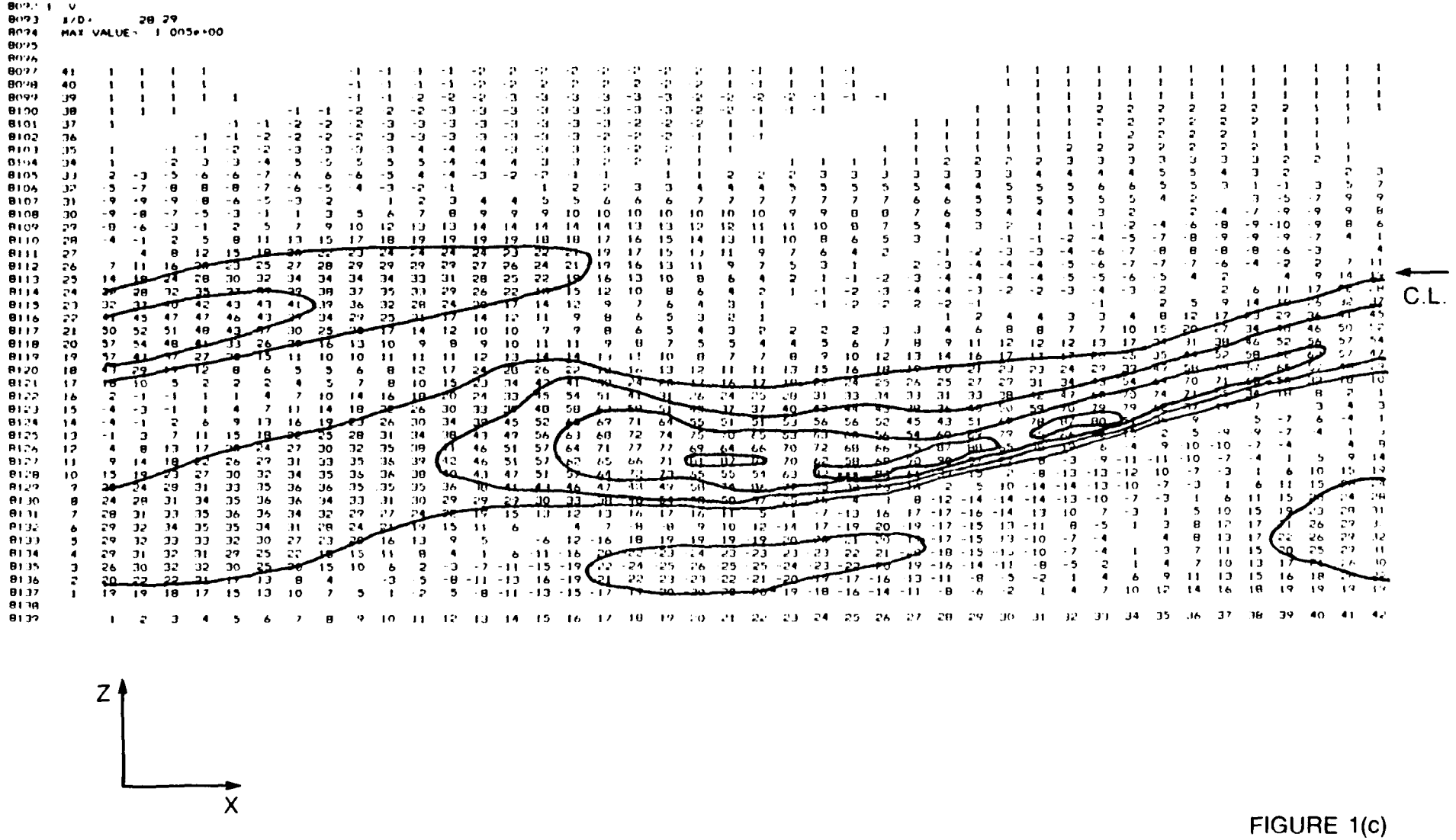

FIGURE 1(c)

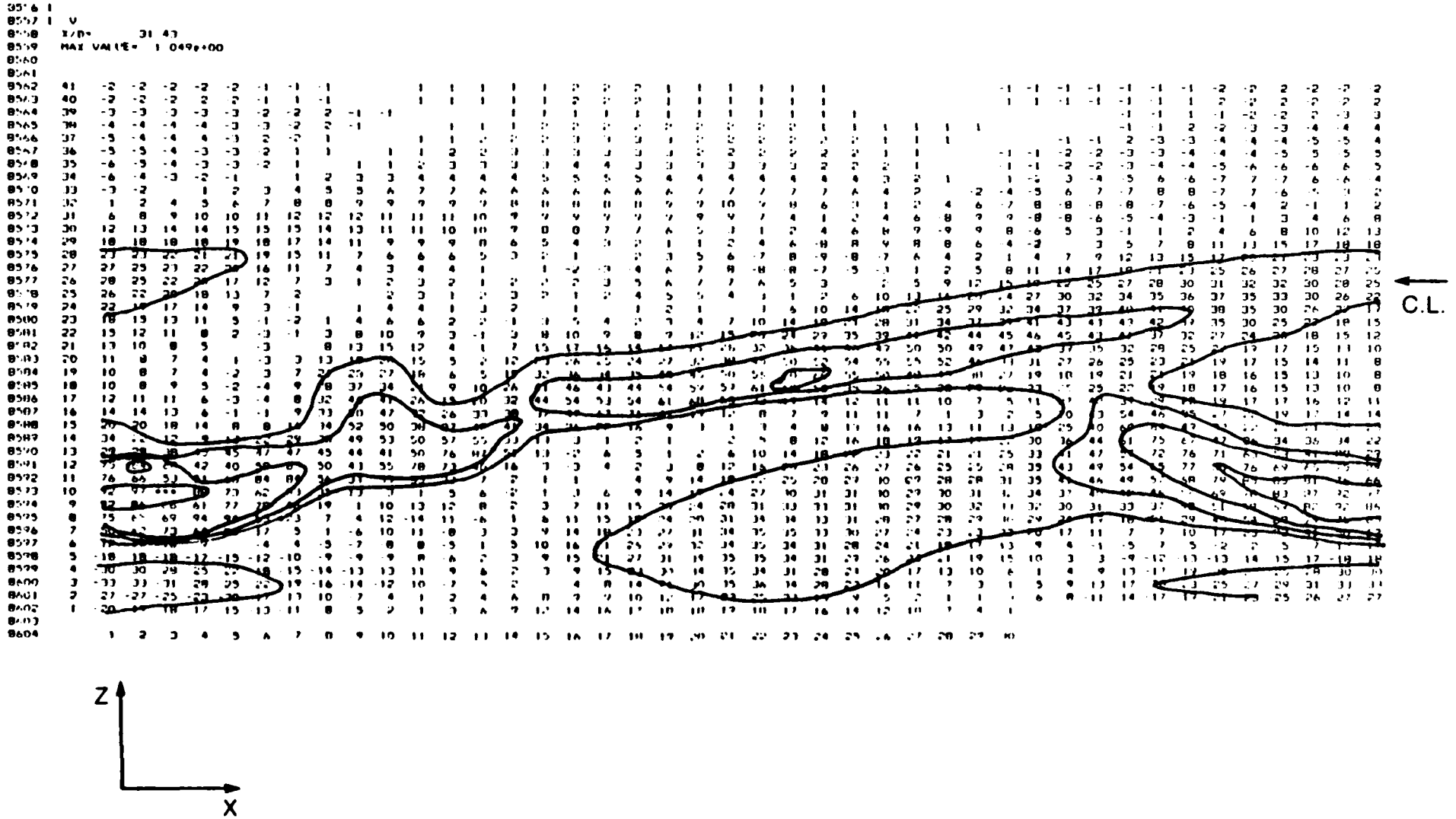

FIGURE 1(d)

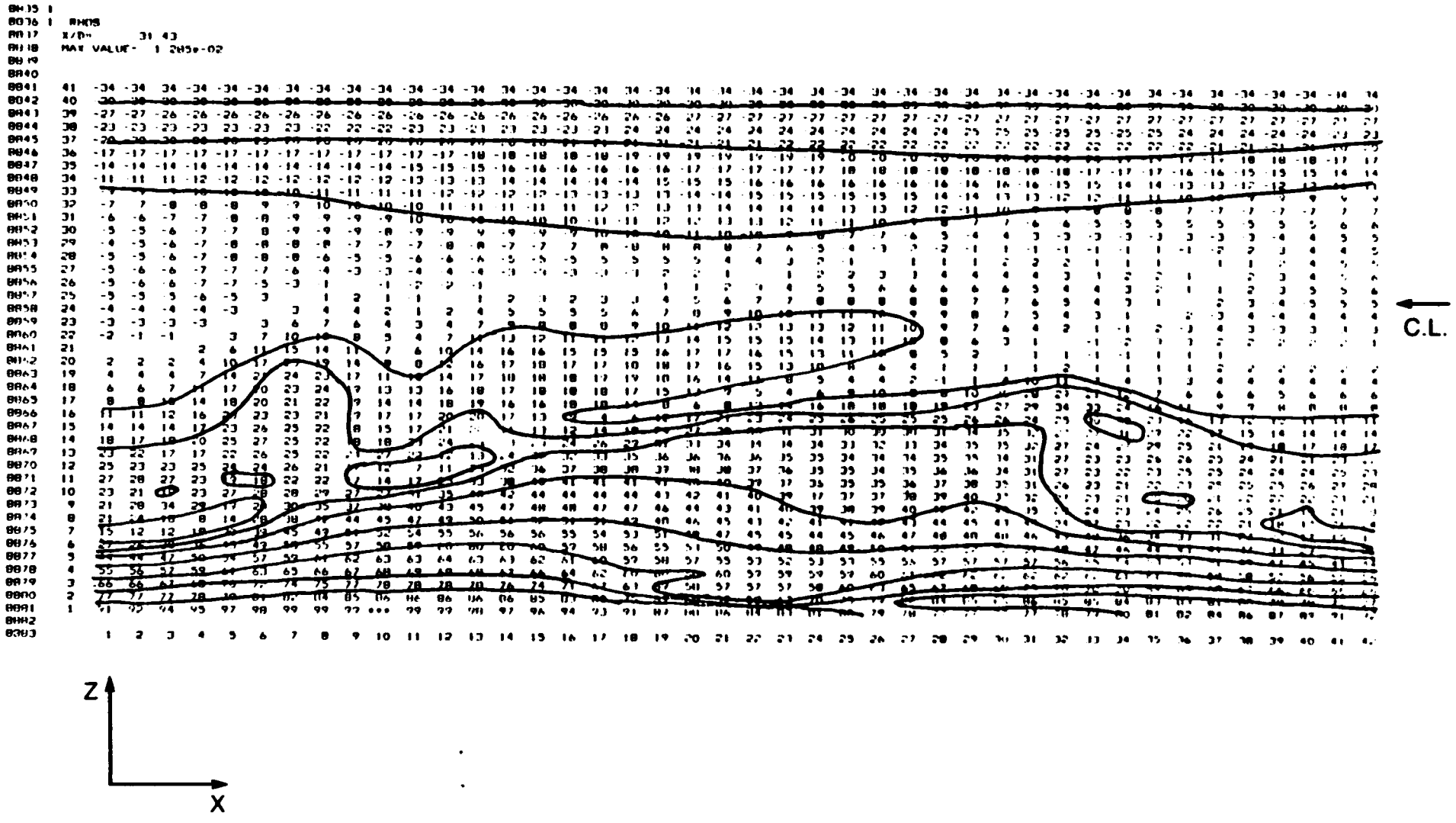

FIGURE 2

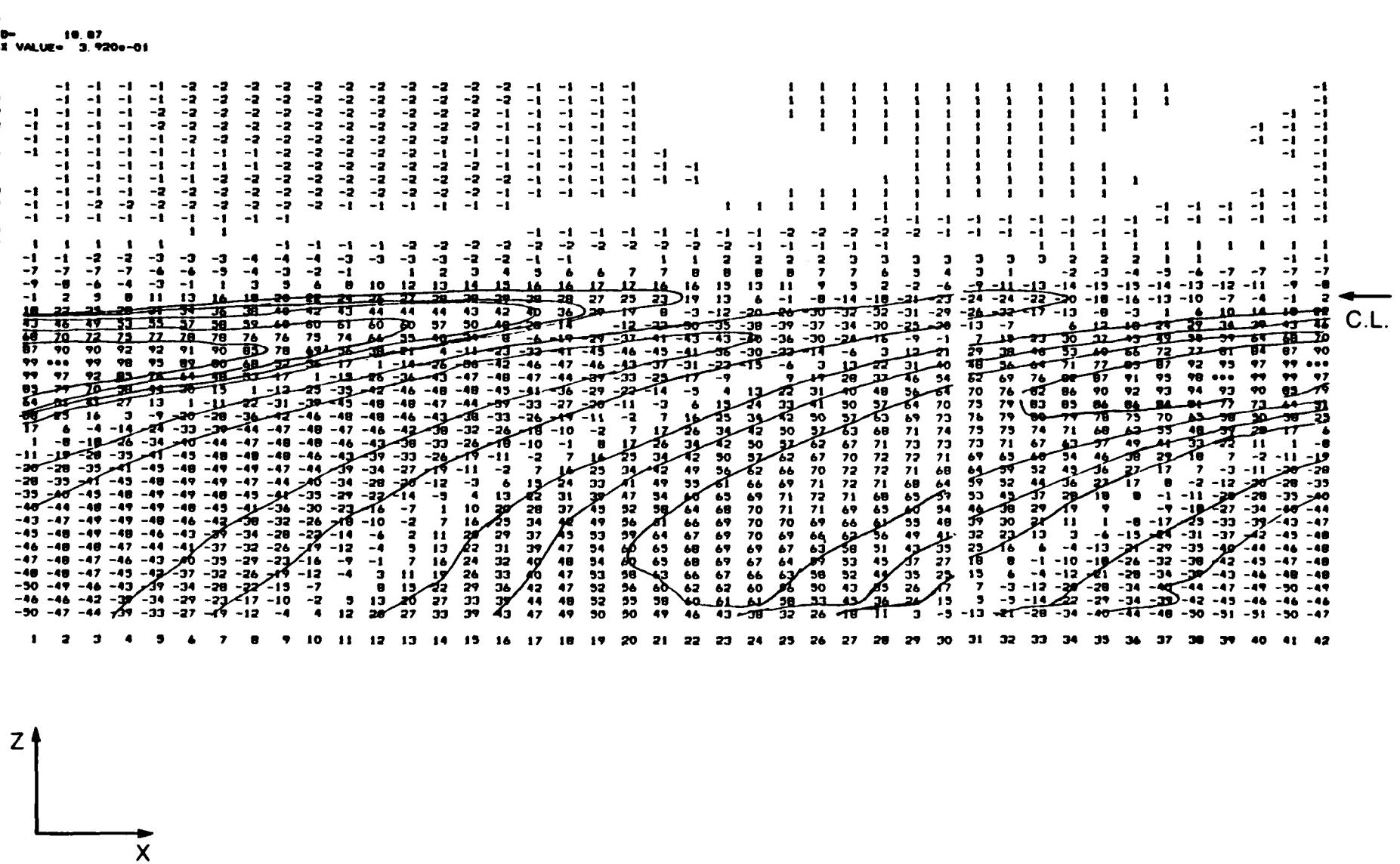

FIGURE 3(a)

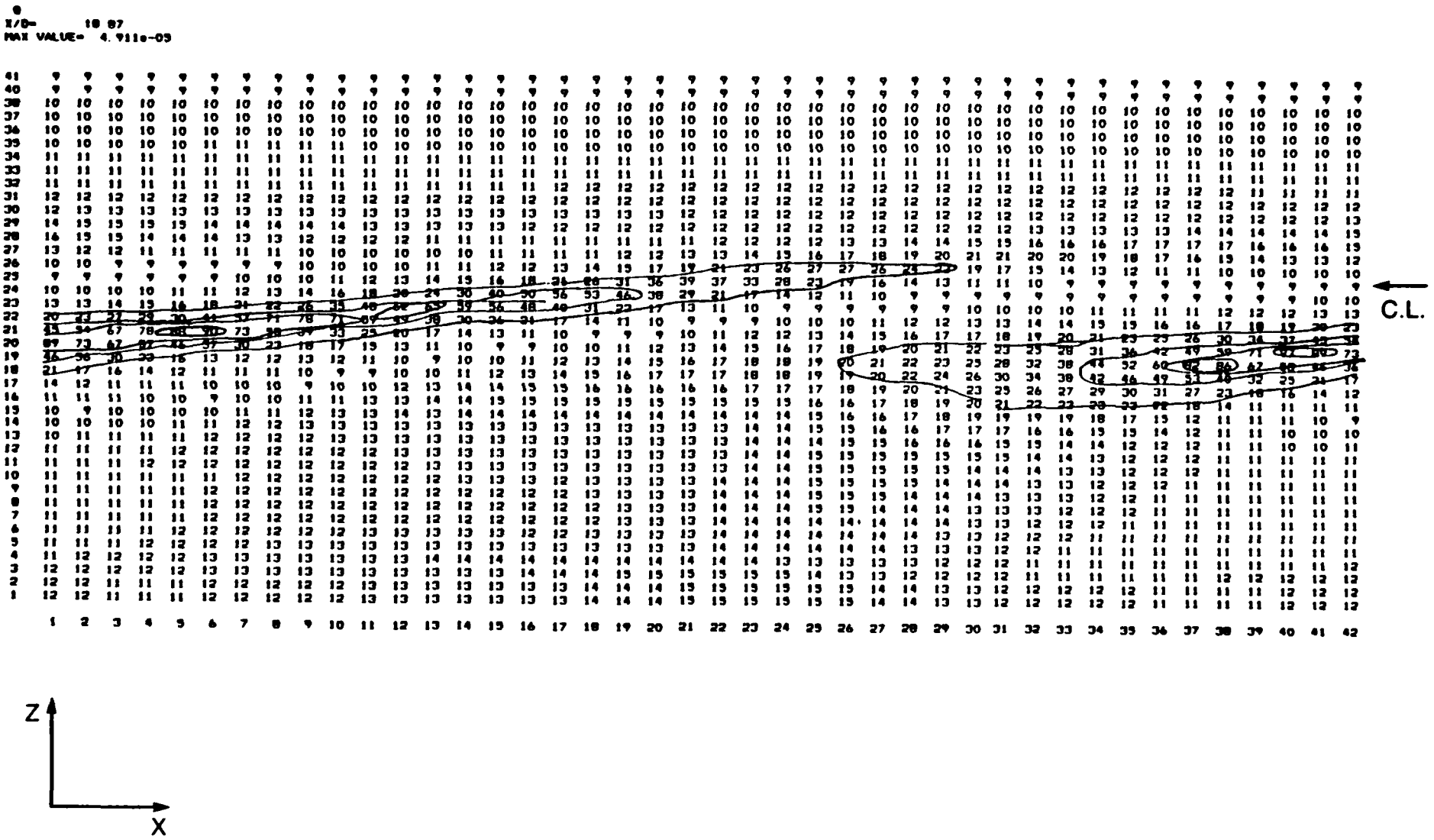

FIGURE 3(b)

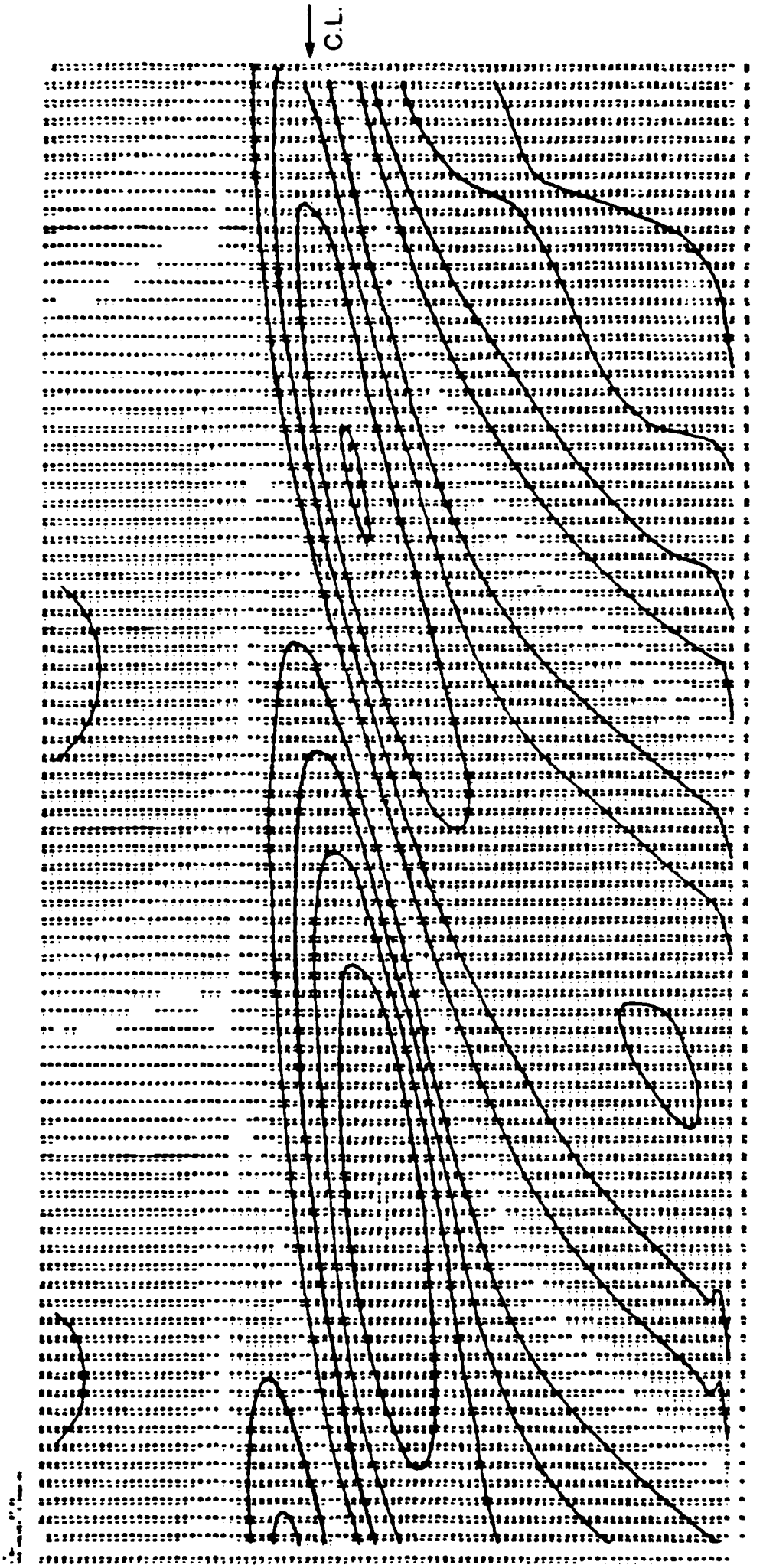

FIGURE 4(a)

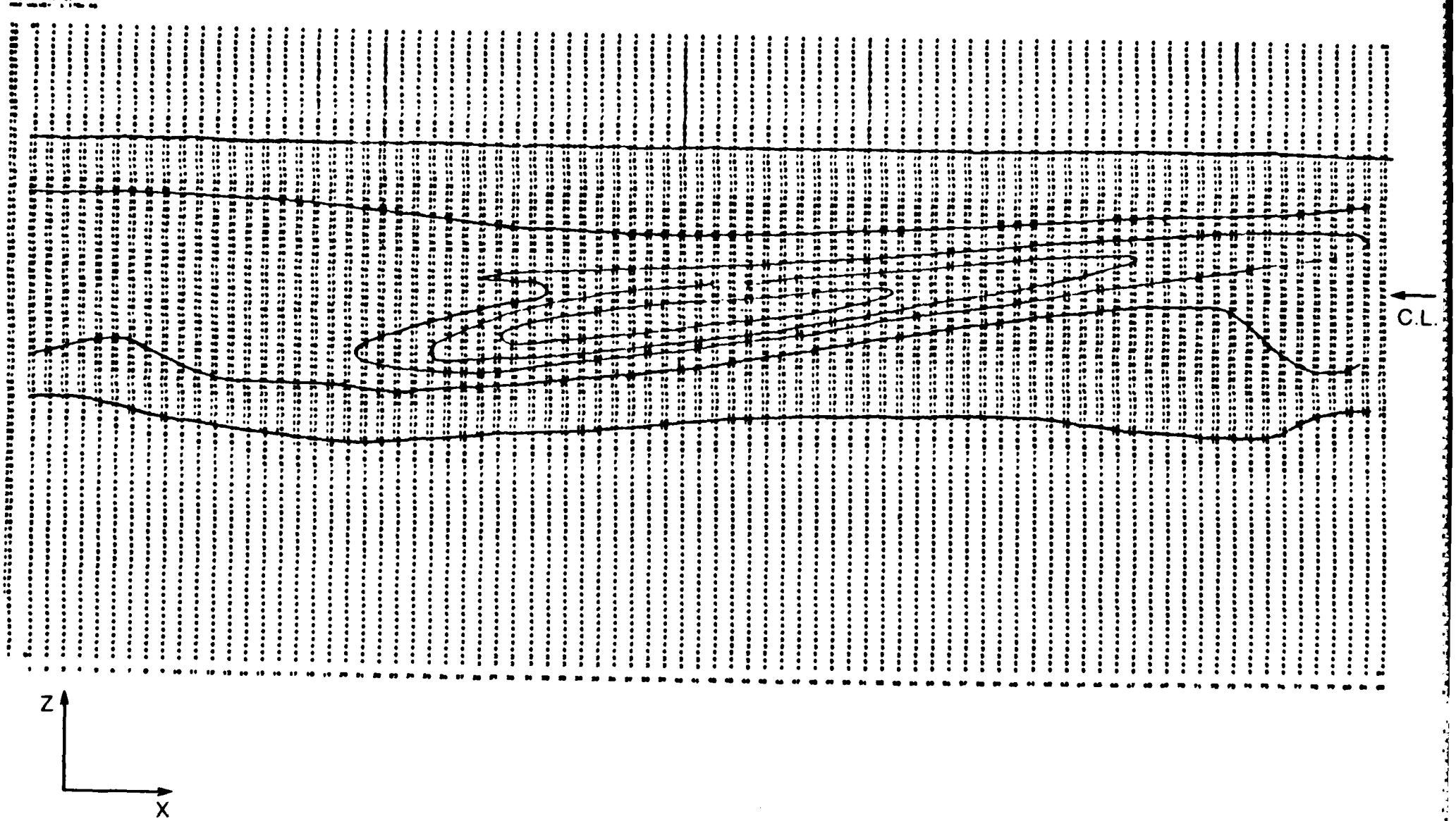

FIGURE 4(b)

END

FILMED

1-86

DTIC